Upper critical fields and interface transparency in superconductor/ferromagnet bilayers

A. Angrisani Armenio, C. Cirillo, G. Iannone, S. L. Prischepa,* and C. Attanasio†
Laboratorio Regionale SuperMat, CNR-INFM Salerno, and Dipartimento di Fisica "E. R. Caianiello," Università degli Studi di Salerno, Baronissi, Salerno I-84081, Italy

(Received 23 November 2006; revised manuscript received 8 February 2007; published 24 July 2007)

Proximity effect in $Nb/Pd_{0.86}Ni_{0.14}$, $Nb/Cu_{0.46}Ni_{0.54}$, and $Nb/Cu_{0.42}Ni_{0.58}$ bilayers has been studied in the presence of an external magnetic field. Upper critical field measurements, performed in parallel configuration, reveal a shift of the two-dimensional–three-dimensional crossover temperature, which we relate to the different interface transparencies of the three analyzed systems.

DOI: 10.1103/PhysRevB.76.024515 PACS number(s): 74.45.+c, 74.78.Fk

I. INTRODUCTION

The interplay between a superconductor (S) and a ferromagnet (F) through proximity effect in artificial S/F hybrids has recently attracted much attention, and many papers have been devoted to study both fundamental and applicative aspects of this intriguing research field.[1] This interest has also been encouraged by development of technology and by the use of weak ferromagnetic alloys (e.g., PdNi and CuNi) characterized by a larger value of the magnetic coherence length, ξ_F, allowing one to fabricate heterostructures with thickness accessible to standard deposition techniques.[2,3] One of the peculiarities of S/F multilayers is that the superconducting wave function does not simply decay in the F layer but it oscillates over the characteristic length ξ_F in the direction perpendicular to the interface. As a consequence, the superconducting critical temperature T_c reveals a nonmonotonic behavior as a function of the thickness of the F layer, d_F,[4,5] and even spectacular reentrant superconductivity has been very recently observed experimentally.[6] However, one of the most important ingredients to have good coupling between the S and F (also very relevant in view of possible applications) is the quality of the interfaces, which must be explicitly considered to model the interaction between the layers.[7–9] The parameter which has been added to the proximity effect theory to describe the role of the boundary among different layers is the interface transparency, which has been extensively studied, theoretically and experimentally, for S/F as well as for S/N structures (here N stands for normal metal), in particular, in relation to its influence on the behavior of T_c as a function of d_S (the thickness of the superconducting layer) and d_F (or d_N, the thickness of the normal layer).[7–14] Also relevant is the expected effect of the interfaces on the temperature dependence of the critical magnetic fields in layered structures. In fact, when the field is applied in the direction parallel to layers, the Cooper pairs move crossing the boundaries and, consequently, experiencing the influence of the interface resistance. Despite this fact, only few papers have been devoted to the study of this aspect of the proximity coupling both in S/N[12,15,16] and S/F cases.[17]

In the present paper, we study the behavior of the critical magnetic fields in three different S/F bilayers: $Nb/Pd_{0.86}Ni_{0.14}$, $Nb/Cu_{0.46}Ni_{0.54}$, and $Nb/Cu_{0.42}Ni_{0.58}$. We find that the properties of the boundaries strongly influence the temperature behavior of $H_{c2\|}$. We argue that the study of the proximity effect in external magnetic fields seems to be another tool to get information about the interface properties in layered systems.

II. SAMPLE PREPARATION AND CHARACTERIZATION

Bilayers were grown on Si(100) substrates in a dual source magnetically enhanced dc triode sputtering system equipped with a movable sample holder, which allows one to fabricate eight different samples in the same deposition run. The deposition conditions used for the samples studied in this paper are very similar to those described elsewhere.[10,11] As far as $Pd_{1-x}Ni_x$ is concerned, a target with an atomic percentage $x=0.10$ was used. Due to its peculiar electronic structure, the magnetic properties of the Pd based alloys are extremely sensitive to the concentration of the ferromagnetic component.[18,19] For this reason, the Ni content in our $Pd_{1-x}Ni_x$ films was checked by Rutherford backscattering technique, whose accuracy in the thin film compositional analysis is of the order of 1%. In this way, the Ni percentage was estimated to be $x \approx 0.14$.[10] In the case of $Cu_{1-x}Ni_x$ alloys, the concentration was determined by energy dispersive spectroscopy analysis. The measured Ni contents were equal to the nominal values of the Ni atomic percentage in the starting targets in the limit of the experimental error, estimated to be less than 3%: $Cu_{46}Ni_{54}$ and $Cu_{42}Ni_{58}$. Two different sets of bilayers were prepared for each of the S/F system. In one set, the Nb thickness d_{Nb} is fixed at 30 nm, while the ferromagnetic layer thickness d_F is variable. In the other set, d_F is fixed at 30 nm, while d_{Nb} changes.

To have information about the quality of the interfaces and to calibrate the deposition rates, x-ray reflectivity measurements have been performed on bilayers deliberately fabricated. In Fig. 1, the reflectivity profile of a $sub/Cu_{46}Ni_{54}/Nb$ (where sub denotes the substrate) bilayer with $d_{Nb}=21.5$ nm and $d_{CuNi}=8.2$ nm is shown together with the simulation curve obtained with the Parrat and Nevot-Croce recursion relation.[20,21] The fit also gives information about the presence of interface roughness σ at different interfaces. In this case, both the bottom $sub/Cu_{46}Ni_{54}$ and the $Cu_{46}Ni_{54}/Nb$ boundary have a roughness value of about 0.9 nm. A Nb_2O_5 oxide layer about 2.0 nm thick is also present on the bilayer surface. Comparable values of σ were also estimated for $sub/Cu_{42}Ni_{58}/Nb$ and $sub/Nb/Pd_{0.86}Ni_{0.14}$ bilayers.[10] A detailed structural characterization of Nb based

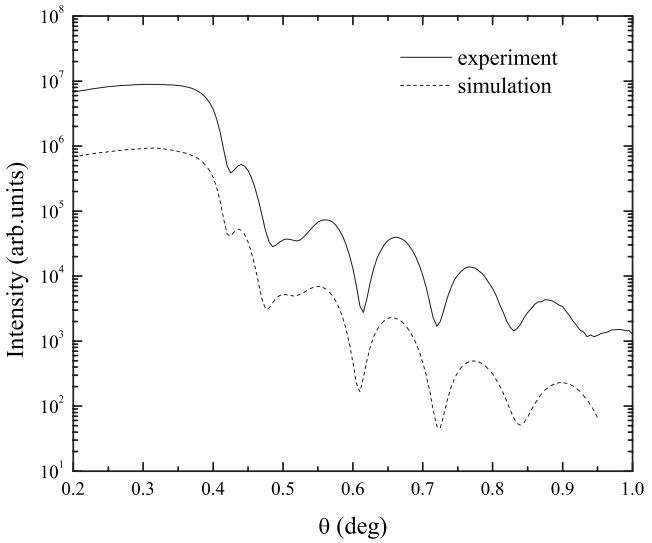

FIG. 1. Experimental (solid line) and calculated (dashed line) low-angle reflectivity profile for a sub/$Cu_{46}Ni_{54}$/Nb bilayer. The numerical simulation is shifted downward for the sake of clarity.

heterostructures, reported in Ref. 12, reveals that these are the typical roughness values of our films. To prevent Nb oxidation in the case of the Nb/$Cu_{1-x}Ni_x$ systems, sub/Nb/$Cu_{1-x}Ni_x$ structures were fabricated, with the top $Cu_{1-x}Ni_x$ acting as a cap layer. The effect of the Nb oxide was instead explicitly taken into account in the interpretation of the results in the case of the measured sub/$Pd_{0.86}Ni_{0.14}$/Nb bilayers.[10] The magnetic properties of the single ferromagnetic films present in our systems have been extensively studied, revealing a well established magnetic ordering at temperatures well above the measured superconducting critical temperature of the bilayers.[22]

III. RESULTS AND DISCUSSION

The superconducting properties, critical temperatures T_c, and critical fields H_{c2}, as a function of the temperature, were resistively measured in a ^{4}He cryostat using a standard dc four-probe technique on unstructured samples 10 mm long and 3 mm wide. The distance between the contact pads, indium welded on the films, was around 2 mm. A bias current of I_{bias}=0.5 mA was used. To avoid thermoelectric offsets, the sign of I_{bias} was reversed at every measurement and the voltage drop was valuated as the average of the difference between the two voltage readings. T_c was taken at 50% of the transition curves, which did not show any hysteretic behaviors, since no difference in the T_c values was observed in the cooling down and in the warming up procedures. The superconducting critical temperatures for Nb/$Cu_{0.46}Ni_{0.54}$ bilayers as a function of d_{Nb} and d_{CuNi} are shown in Figs. 2(a) and 2(b), respectively. The critical temperatures of the samples with $d_{Nb}<25$ nm are not reported since they were below 1.7 K, the lowest temperature reachable in our cryostat. In performing these measurements no field was applied to the samples, which are in a demagnetized state. The error bars are estimated from the difference in temperature at 10%

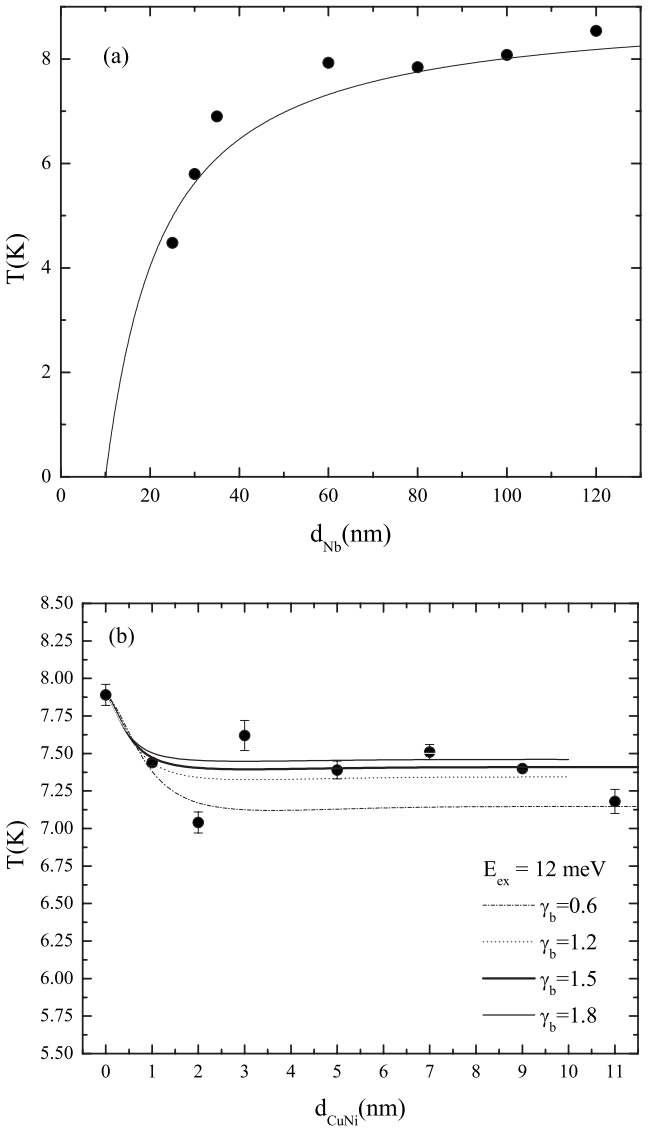

FIG. 2. (a) Superconducting critical temperatures for Nb/$Cu_{0.46}Ni_{0.54}$ bilayers as a function of d_{Nb}, for $d_{Cu_{0.46}Ni_{0.54}}$ =30 nm. The line is the result of the theoretical calculations for γ_b=1.5 and E_{ex}=12 meV. (b) Superconducting critical temperatures for Nb/$Cu_{0.46}Ni_{0.54}$ bilayers as a function of $d_{Cu_{0.46}Ni_{0.54}}$, for d_{Nb} =30 nm. Different lines (dotted, light and thick solid, and dot-dashed) are the results of the theoretical fit for different values of γ_b and for E_{ex}=12 meV. All the microscopical parameters used in the model are given in the text.

and 90% of the transitions. Similar T_c behavior has been obtained also for Nb/$Cu_{0.42}Ni_{0.58}$ and Nb/$Pd_{0.86}Ni_{0.14}$ bilayers.[10] Following the same procedure used in Ref. 10, we analyzed the behavior of both $T_c(d_F)$ and $T_c(d_S)$ in the framework of the theoretical model developed by Fominov *et al.*[9] In the single-mode approximation, the critical temperature of our bilayers is obtained from the following equations:[9,10]

$$\ln\left(\frac{T_{cS}}{T_c}\right) = \Psi\left(\frac{1}{2} + \frac{\Omega_0^2}{2}\frac{T_{cS}}{T_c}\right) - \Psi\left(\frac{1}{2}\right), \qquad (1)$$

$$\Omega_0 \tan\left(\Omega_0 \frac{d_S}{\xi_S}\right) = \gamma \frac{A_S(\gamma_b + \mathrm{Re}\, B_F) + \gamma}{A_S|\gamma_b + B_F|^2 + \gamma(\gamma_b + \mathrm{Re}\, B_F)}, \quad (2)$$

where, due to the single-mode approximation, only the real root Ω_0 of Eq. (1) is considered. Here,

$$B_F = [k_F \xi_F^* \tanh(k_F d_F)]^{-1}, \quad k_F = \frac{1}{\xi_F^*} \sqrt{\frac{|\pi k_B T_c| + iE_{ex}}{\pi k_B T_{cS}}}, \quad (3)$$

$$A_S = k_S \xi_S \tanh(k_S d_S), \quad k_S = \frac{1}{\xi_S} \sqrt{\frac{T_c}{T_{cS}}}. \quad (4)$$

$$\gamma = \frac{\rho_S \xi_S}{\rho_F \xi_F^*}, \quad (5)$$

where $\Psi(x)$ is the digamma function, T_{cS} is the critical temperature of the single S layer, and $\rho_{S,F}$ are the low-temperature resistivities.

The parameter γ_b describes the quality of the barrier, being related to the interface transparency $\mathcal{T}$ through the expression

$$\gamma_b = \frac{2}{3} \frac{l_F}{\xi_F^*} \frac{1 - \mathcal{T}}{\mathcal{T}}. \quad (6)$$

In previous equations, the superconducting and ferromagnetic coherence lengths appear, which can be expressed respectively as follows:

$$\xi_S = \sqrt{\frac{\hbar D_S}{2\pi k_B T_{cS}}}, \quad (7)$$

$$\xi_F^* = \sqrt{\frac{\hbar D_F}{2\pi k_B T_{cS}}}. \quad (8)$$

Here, $D_{S,F}$ are the diffusion coefficients of S and F. ξ_S is related to the Ginzburg-Landau (GL) coherence length ξ_0 by the relation $\xi_S = 2\xi_0/\pi$, while ξ_F^* is a measure of the diffusive motion of the Cooper pairs in the ferromagnet and should not be confused with $\xi_F = \sqrt{\hbar D_F / E_{ex}}$, which instead measures both the decay and the oscillation length of the order parameter in F. A large number of microscopical parameters appear in the model, but part of them can be derived independently.[10] The diffusion coefficients $D_{S,F}$ are related to the low-temperature resistivities $\rho_{S,F}$ through the electronic mean free paths $l_{S,F}$ by[23]

$$D_{S,F} = \frac{v_{S,F} l_{S,F}}{3}, \quad (9)$$

in which

$$l_{S,F} = \frac{1}{v_{S,F} \gamma_{S,F} \rho_{S,F}} \left(\frac{\pi k_B}{e}\right)^2, \quad (10)$$

where $\gamma_{S,F}$ are the electronic specific heat coefficients and $v_{S,F}$ are the Fermi velocities. The values for T_{cS}, the critical temperature of a single Nb film 30 nm thick, is equal to 7.89 K, while for its resistivity a value of 17 $\mu\Omega$ cm has been measured. In this way, using $\gamma_{Nb} \approx 7 \times 10^{-4}$ J/K^2 cm^3 (Ref. 24) and $v_{Nb} = 2.73 \times 10^7$ cm/s,[25] the Nb coherence length has been evaluated from Eq. (7) to be $\xi_{Nb} = 5.6$ nm.[23] The measured values for the low-temperature resistivities of the magnetic films 60 nm thick are $\rho_{Pd_{0.86}Ni_{0.14}} = 20$ $\mu\Omega$ cm, $\rho_{Cu_{0.46}Ni_{0.54}} = 50$ $\mu\Omega$ cm, and $\rho_{Cu_{0.42}Ni_{0.58}} = 55$ $\mu\Omega$ cm. In these cases, however, we assume the ferromagnetic mean free path to be thickness limited, using an average value of $l_F \approx 4$ nm. This assumption is due to the fact that the low-temperature resistivity of the alloys drastically increases for films thinner than 10 nm,[26] so the $\rho_F(d_F)$ dependence should be taken in to account to reproduce the experimental data. In addition, in order to apply relations (9) and (10), the electronic specific heat coefficients and the Fermi velocities of the alloys should be known. In our approximation from Eq. (8), we get $\xi^*_{Pd_{0.86}Ni_{0.14}} = 6.8$ nm, $\xi^*_{Cu_{0.46}Ni_{0.54}} = 5.9$ nm, and $\xi^*_{Cu_{0.42}Ni_{0.58}} = 6.2$ nm. At this point, the values of the exchange energy E_{ex} and of γ_b for the three systems are the only fitting parameters in the model.

In the simulation procedure, the γ_b value was determined from the vertical position of the $T_c(d_F)$ curve, while E_{ex} was selected to better reproduce the saturation set in. For $Nb/Pd_{0.86}Ni_{0.14}$, we get $\gamma_b = 0.6$ and $E_{ex} = 13$ meV,[10] while for both the $Nb/Cu_{1-x}Ni_x$ systems, we obtained very similar values: $\gamma_b = 1.5$ and $E_{ex} = 12$ meV. The comparable values of E_{ex} estimated for the three alloys suggest that the suppression of the superconducting ordering due to the presence of the different ferromagnets on the Nb in the bilayers is almost equivalent. The results of the theoretical simulations obtained for the $Nb/Cu_{46}Ni_{54}$ system with the same values for both the fixed and fitting parameters are shown as lines in Figs. 2(a) and 2(b). In Fig. 2(b), the best fit curve is reported, together with three more simulations obtained for different values of γ_b. The values of the root mean square (rms) associated with the different curves were also considered. The minimum rms=0.17 was obtained for $\gamma_b = 1.5$. Taking into account the spreading of the experimental data and the rms value, we estimated the fitting parameter to be $\gamma_b = 1.5 \pm 0.3$. Despite the significant data scattering, it is evident that the $T_c(d_F)$ dependence cannot be described by the lower γ_b value estimated for the $Nb/Pd_{0.86}Ni_{0.14}$ bilayers [dashed-dotted line in Fig. 2(b)], as also suggested by the higher value of the rms for this curve (rms=0.26). We finally obtain $\gamma_b = 1.5 \pm 0.3$ and $E_{ex} = 12 \pm 2$ meV for both the $Nb/Cu_{1-x}Ni_x$ systems and $\gamma_b = 0.60 \pm 0.15$ and $E_{ex} = 13 \pm 2$ meV for $Nb/Pd_{0.86}Ni_{0.14}$.[10] These results point out that the interface transparency of our $Nb/Cu_{1-x}Ni_x$ interface is lower compared with that of $Nb/Pd_{0.86}Ni_{0.14}$. This conclusion is in agreement with other data presented in the literature.[9,26]

Even though the presence of a crossover phenomenon in the temperature dependence of the critical field has been studied extensively in the past,[27,28] the role of the interface transparency and its influence on $H_{c2\|}(T)$ has been experimentally studied only in the case of S/N hybrids, namely, Cu/Nb/Cu triple layers, obtained with different deposition techniques.[12] It was observed that, according to theoretical predictions,[16] the two-dimensional–three-dimensional (2D-3D) crossover temperature moves toward a lower value in the case of higher interface transparency. Interestingly, this

TABLE I. Characteristic parameters of the investigated bilayers. d_S (d_F) is the thickness of the superconducting (ferromagnetic) layer, T_c is the critical temperature, and t_{cr} is the crossover temperature. d_{eff} is the sample's effective thickness.

Sample	Name	d_S (nm)	d_F (nm)	T_c (K)	t_{cr}	d_{eff} (nm)
$Nb/Pd_{0.86}Ni_{0.14}$	NP14	30	30	5.67	0.675	9.6
$Nb/Cu_{0.46}Ni_{0.54}$	NC54	30	30	5.49	0.836	12.8
$Nb/Cu_{0.42}Ni_{0.58}$	NC58	30	30	5.00	0.820	10.6

result was obtained only for smaller values of d_{Nb} when the role played by the S/N interfaces is more relevant.[12] For this reason, among the samples of the series with fixed d_F (d_F =30 nm), we have measured the temperature dependence of the parallel critical magnetic field for the samples with the thinnest Nb thickness, namely, d_{Nb}=30 nm. The choice of d_F=30 nm was instead motivated by the fact that, at this thickness value, a saturated $T_c(d_F)$ behavior is recovered. In this regime, the jump of the pair amplitude at the S/F boundary, due to the fulfillment of the quantum boundary conditions, is constant, signature of a constant flux of Cooper pairs coming from the S layer.[8] This condition enables us to compare the results obtained for the different systems, interpreting them only in terms of the different qualities of the barriers. For the sake of clarity, in the following, we will name these samples using the letters NP or NC, according to whether the ferromagnetic metal is, respectively, $Pd_{1-x}Ni_x$ or $Cu_{1-x}Ni_x$, followed by a number indicating the Ni content of the alloy. For example, NP14 is the $Nb/Pd_{0.86}Ni_{0.14}$ bilayer, while NC58 is the $Nb/Cu_{0.42}Ni_{0.58}$ one. The samples' names and properties are summarized in Table I. The three samples have comparable values of the critical temperature because of the similar Nb quality in all the systems. In Fig. 3, the temperature behavior of the perpendicular, $\mu_0 H_{c2\perp}$, and of the parallel, $\mu_0 H_{c2\parallel}$, critical magnetic fields for the sample NC58 are reported. $\mu_0 H_{c2\parallel}(T)$ dependence at high temperature is well described by a square-root fit (light line) down to T=4.94 K, namely, $t=T/T_c=0.99$. The only point which deviates from the curve is that for $T=T_c$, which we believe is not related to a further crossover. On the other hand, at lower temperatures the experimental data follow a linear fit (thick line). In fact, an overall square-root fit of the data gives a value of $\chi^2=1.42\times10^{-3}$, while the linear fit at low temperatures gives $\chi^2=0.08\times10^{-3}$, confirming that the low-temperature data are better described by a linear relation. The temperature at which the change in the $\mu_0 H_{c2\parallel}(T)$ dependence sets in indicates the crossover temperature T_{cr} between a 3D regime, where $\mu_0 H_{c2\parallel}$ is linear, and a 2D regime at higher temperatures. It is also worthy to mention that the presence of surface superconductivity can be excluded since the ratio $H_{c2\parallel}/H_{c2\perp}$ is always higher than 1.7. In Fig. 4, the $\mu_0 H_{c2\parallel}(t)$ dependence is reported for the three S/F bilayers, together with the indication of the reduced temperature crossover, $t_{cr}=T_{cr}/T_c$. The observed behavior is typical of a single Nb film measured in parallel field.[29] In fact, at lower temperatures, when $\xi_\perp(T)<d_{Nb}$, the film behaves like a 3D system, while close to T_c, where $\xi_\perp(T)$ diverges, $\xi_\perp(T)$

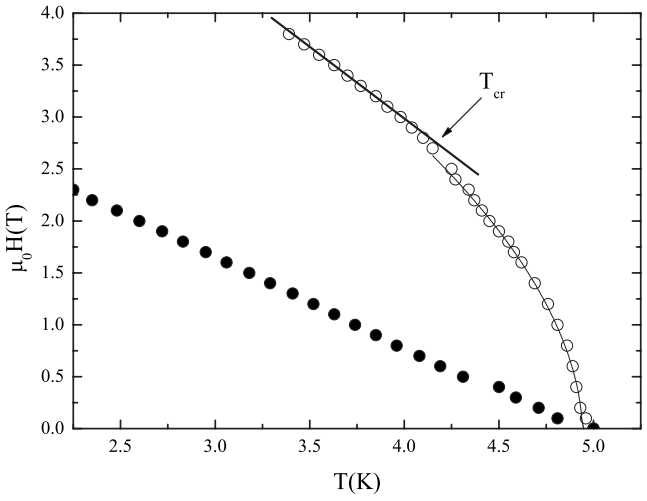

FIG. 3. Temperature dependence of the parallel (open circles) and perpendicular (filled circles) critical magnetic fields for a $Nb/Cu_{0.42}Ni_{0.58}$ bilayer with $d_{Nb}=d_{Cu_{0.42}Ni_{0.58}}$=30 nm. The light line (thick) describes the 3D (2D) $\mu_0 H_{c2\parallel}(T)$ behavior. The arrow indicates the crossover temperature T_{cr}.

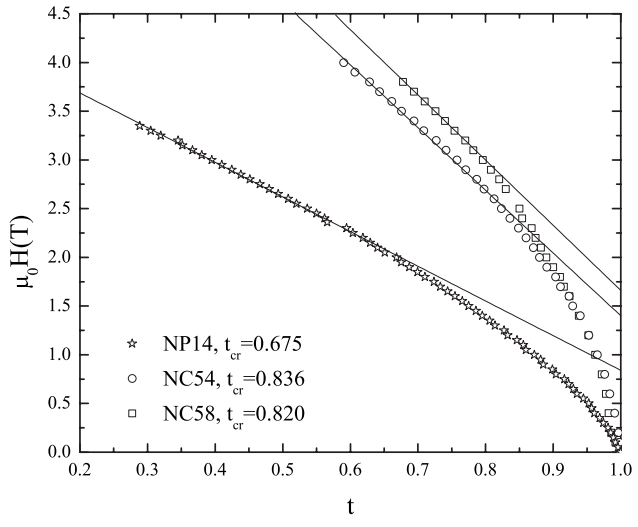

FIG. 4. Parallel critical magnetic fields as a function of the reduced temperature for the three analyzed bilayers with $d_S=d_F$ =30 nm: $Nb/Cu_{0.42}Ni_{0.58}$ (squares), $Nb/Cu_{0.46}Ni_{0.54}$ (circles), and $Nb/Pd_{0.86}Ni_{0.14}$ (stars). The straight lines show the linear 3D behavior below t_{cr}. The numbers indicate the values of the t_{cr} for the three different systems.

$>d_{\mathrm{Nb}}$ and the 2D dependence is observed ($\xi_\perp$ is the GL coherence length perpendicular to the plane of the layer). Also in these cases, the χ^2 test confirms that the low-temperature data are better reproduced by a linear fit than by a square-root dependence. We believe that the difference in the crossover temperature is related to the different qualities of the interface transparency in the three S/F systems. Our S/F bilayers, in fact, may be considered as single superconducting films having a smaller "effective thickness," d_{eff}, because at the S/F interface, superconductivity is destroyed due to the proximity effect. For this reason, the higher the transparency of the barrier, the thinner is d_{eff}. Consequently, for high $\mathcal{T}$ values, the 3D-2D crossover moves toward lower temperatures, because the condition $\xi_\perp < d_{eff}$ is fulfilled in a smaller temperature region.

The behavior of the parallel critical field, in the 3D regime when $\xi_\perp(T) < d_S$, is described by the equation[30]

$$\mu_0 H_{c2\parallel}(T) = \frac{\phi_0}{2\pi\xi_\parallel(0)\xi_\perp(0)}\left(1-\frac{T}{T_c}\right), \tag{11}$$

while in the 2D regime for $\xi_\perp(T) > d_S$, $\mu_0 H_{c2\parallel}$ is described by the Tinkham expression[30]

$$\mu_0 H_{c2\parallel}(T) = \frac{\sqrt{12}\phi_0}{2\pi\xi_\parallel(0)d}\sqrt{1-\frac{T}{T_c}}. \tag{12}$$

Here, $\xi_\parallel(0)$ $[\xi_\perp(0)]$ is the zero temperature value of the GL coherence length parallel (perpendicular) to the plane of the layers, ϕ_0 is the superconducting quantum flux, and d is the sample thickness.

The perpendicular critical magnetic field for a superconducting film with arbitrary thickness d_S always shows a linear temperature dependence, given by

$$\mu_0 H_{c2\perp}(T) = \frac{\phi_0}{2\pi\xi_\parallel^2(0)}\left(1-\frac{T}{T_c}\right). \tag{13}$$

By a linear extrapolation of the measured critical magnetic fields down to zero temperature, we have obtained, using Eqs. (11) and (13), the values for $\xi_\perp(0)$ for the three bilayers: $\xi_\perp^{NP14}(0)=5.5$ nm, $\xi_\perp^{NC54}(0)=5.2$ nm, and $\xi_\perp^{NC58}(0)=4.5$ nm. Moreover, since t_{cr} is defined as the temperature at which the dimensional crossover occurs, it follows that d_{eff} is given by $d_{eff}\approx\xi_\perp(t_{cr})$. In this way, the values of the superconductors' effective thicknesses in the different systems were estimated, giving $d_{eff}^{NP14}=9.6$ nm, $d_{eff}^{NC54}=12.8$ nm, and $d_{eff}^{NC58}=10.6$ nm. Therefore, this result, $d_{eff}^{NP14}<d_{eff}^{NC54},d_{eff}^{NC58}$, confirms the higher quality of the $Nb/Pd_{0.86}Ni_{0.14}$ barriers, in accordance with the T_c measurements. It is interesting to note that the analyzed samples are characterized by comparable values of the physical parameters (T_{cS}, ξ_F, E_{ex}, and resistivities). In addition, as previously mentioned, the Nb qualities in three bilayers are very similar. Therefore we believe that the different t_{cr} values are mainly due to the different interface transparencies of the three systems.

IV. CONCLUSIONS

In conclusion, we have studied the influence of the interface transparency on upper critical magnetic field measurements in different S/F bilayers. We found that the properties of the barrier strongly influence the temperature dependence of $H_{c2\parallel}$. In particular, the temperature at which the 2D-3D crossover takes place moves toward lower temperatures for higher values of the interface transparency. Even tough we are not able to extract any number for γ_b from this procedure, the differences in t_{cr} are very pronounced. For this reason, we believe that the study of the S/F proximity effect in external fields could give useful information about the properties of the interfaces.

*Permanent address: Belarus State University of Informatics and Radio Electronics, P. Brovka Street 6, 220013 Minsk, Belarus.
†Corresponding author. FAX: +39-089-965275. attanasio@sa.infn.it

[1] A. I. Buzdin, Rev. Mod. Phys. **77**, 935 (2005).
[2] T. Kontos, M. Aprili, J. Lesueur, and X. Grison, Phys. Rev. Lett. **86**, 304 (2001).
[3] V. V. Ryazanov, V. A. Oboznov, A. Yu. Rusanov, A. V. Veretennikov, A. A. Golubov, and J. Aarts, Phys. Rev. Lett. **86**, 2427 (2001).
[4] I. A. Garifullin, J. Magn. Magn. Mater. **240**, 571 (2002).
[5] I. A. Garifullin, D. A. Tikhonov, N. N. Garif'yanov, L. Lazar, Yu. V. Goryunov, S. Ya. Khlebnikov, L. R. Tagirov, K. Westerholt, and H. Zabel, Phys. Rev. B **66**, 020505(R) (2002).
[6] V. Zdravkov, A. Sidorenko, G. Obermeier, S. Gsell, M. Schreck, C. Müller, S. Horn, R. Tidecks, and L. R. Tagirov, Phys. Rev. Lett. **97**, 057004 (2006).
[7] J. Aarts, J. M. E. Geers, E. Brück, A. A. Golubov, and R. Coehoorn, Phys. Rev. B **56**, 2779 (1997).
[8] L. R. Tagirov, Physica C **307**, 145 (1998).
[9] Ya. V. Fominov, N. M. Chtchelkatchev, and A. A. Golubov, Phys. Rev. B **66**, 014507 (2002).
[10] C. Cirillo, S. L. Prischepa, M. Salvato, C. Attanasio, M. Hesselberth, and J. Aarts, Phys. Rev. B **72**, 144511 (2005).
[11] C. Cirillo, S. L. Prischepa, M. Salvato, and C. Attanasio, Eur. Phys. J. B **38**, 59 (2004).
[12] A. Tesauro, A. Aurigemma, C. Cirillo, S. L. Prischepa, M. Salvato, and C. Attanasio, Supercond. Sci. Technol. **18**, 152 (2005).
[13] V. N. Kushnir, S. L. Prischepa, C. Cirillo, and C. Attanasio, Eur. Phys. J. B **52**, 9 (2006).
[14] L. R. Tagirov and N. Garcia, Superlattices Microstruct. **41**, 152 (2007).
[15] C. Ciuhu and A. Lodder, Superlattices Microstruct. **30**, 95 (2001).
[16] C. Ciuhu and A. Lodder, Phys. Rev. B **64**, 224526 (2001).
[17] B. Krunavakarn and S. Yoksan, Physica C **440**, 25 (2006).
[18] G. J. Nieuwenhuys, Adv. Phys. **24**, 515 (1975).
[19] J. Beille, Ph.D. thesis, Université Joseph Fourier, 1975.
[20] L. G. Parrat, Phys. Rev. **95**, 359 (1954).

[21] L. Nevot and P. Croce, Rev. Phys. Appl. **15**, 761 (1980).
[22] G. Iannone, D. Zola, A. Angrisani Armenio, M. Polichetti, and C. Attanasio, Phys. Rev. B **75**, 064409 (2007).
[23] J. J. Hauser, H. C. Theurer, and N. R. Werthamer, Phys. Rev. **136**, A637 (1964).
[24] *Handbook of Chemistry and Physics*, edited by R. C. Weast (Chemical Rubber, Cleveland, 1972).
[25] H. R. Kerchner, D. K. Christen, and S. T. Sekula, Phys. Rev. B **24**, 1200 (1981).
[26] C. Cirillo, A. Rusanov, C. Bell, and J. Aarts, Phys. Rev. B **75**, 174510 (2007).
[27] V. I. Dediu, V. V. Kabanov, and A. S. Sidorenko, Phys. Rev. B **49**, 4027 (1994).
[28] V. N. Kushnir, S. L. Prischepa, C. Cirillo, M. L. Della Rocca, A. Angrisani Armenio, L. Maritato, M. Salvato, and C. Attanasio, Eur. Phys. J. B **41**, 439 (2004).
[29] M. Schöck, C. Sürgers, and H. v. Löhneysen, Eur. Phys. J. B **14**, 1 (2000).
[30] B. Y. Jin and J. B. Ketterson, Adv. Phys. **38**, 189 (1989).